



IMMUNOPATHOLOGY AND INFECTIOUS DISEASES

Serum Amyloid P and a Dendritic Cell–Specific Intercellular Adhesion Molecule-3–Grabbing Nonintegrin Ligand Inhibit High-Fat Diet–Induced Adipose Tissue and Liver Inflammation and Steatosis in Mice



Darrell Pilling, Nehemiah Cox, Megan A. Thomson, Tejas R. Karhadkar, and Richard H. Gomer

From the Department of Biology, Texas A&M University, College Station, Texas

Accepted for publication
August 20, 2019.

Address correspondence to:
Darrell Pilling, Ph.D., or
Richard H. Gomer, Ph.D.,
Department of Biology, Texas
A&M University, 301 Old
Main Dr., 3474 TAMU, Col-
lege Station, TX 77843-
3474. E-mail: dpilling@bio.tamu.edu
or rgomer@tamu.edu.

High-fat diet (HFD)–induced inflammation is associated with a variety of health risks. The systemic pentraxin serum amyloid P (SAP) inhibits inflammation. SAP activates the high-affinity IgG receptor Fcγ receptor I (FcγRI; CD64) and the lectin receptor dendritic cell–specific intercellular adhesion molecule-3–grabbing nonintegrin (DC-SIGN; CD209). Herein, we show that for mice on an HFD, injections of SAP and a synthetic CD209 ligand (1866) reduced HFD-increased adipose and liver tissue inflammation, adipocyte differentiation, and lipid accumulation in adipose tissue. HFD worsened glucose tolerance test results and caused increased adipocyte size; for mice on an HFD, SAP improved glucose tolerance test results and reduced adipocyte size. Mice on an HFD had elevated serum levels of IL-1β, IL-23, interferon (IFN)-β, IFN-γ, monocyte chemoattractant protein 1 [MCP-1; chemokine (C-C motif) ligand 2 (CCL2)], and tumor necrosis factor-α. SAP reduced serum levels of IL-23, IFN-β, MCP-1, and tumor necrosis factor-α, whereas 1866 reduced IFN-γ. *In vitro*, SAP, but not 1866, treated cells isolated from white fat tissue (stromal vesicular fraction) produced the anti-inflammatory cytokine IL-10. HFD causes steatosis, and both SAP and 1866 reduced it. Conversely, compared with control mice, SAP knockout mice fed on a normal diet had increased white adipocyte cell sizes, increased numbers of inflammatory cells in adipose and liver tissue, and steatosis; and these effects were exacerbated on an HFD. SAP and 1866 may inhibit some, but not all, of the effects of a high-fat diet. (*Am J Pathol* 2019, 189: 2400–2413; <https://doi.org/10.1016/j.ajpath.2019.08.005>)

Obesity is the excessive accumulation of fat in the body due to a net excess of calories, and in the United States, more than one-third of adults are obese.¹ Obesity is associated with heart disease, type 2 diabetes, and chronic liver disease, and the estimated annual medical cost of obesity in the United States was approximately \$147 billion/year in 2008.² Obesity induces adipocyte metabolic dysregulation and the production of inflammatory cytokines, leading to systemic metabolic dysregulation, such as the inability to effectively regulate systemic glucose levels (insulin resistance), elevated lipid levels (dyslipidemia), and immune cell recruitment to, and activation in, adipose tissue and liver (inflammation).³ Excess calories leads to elevated circulating levels of glucose and free fatty acids, which force

adipocytes to accumulate more lipid and expand in size, leading to increased oxidative stress in adipocytes and local hypoxia of the tissue, because of the inability of oxygen to diffuse across the tissue.^{3,4} These processes lead to adipocyte cell death, initiating the activation of adipose tissue macrophages.^{4,5} In the liver, excess calories lead to Kupffer cell (hepatic macrophage) activation, which then promotes

Supported by NIH grant HL118507 (R.H.G.).

Disclosures: D.P. and R.H.G. are cofounders of and have equity in Promedior, a company that is developing SAP as a therapeutic; D.P. and R.H.G. receive a share of royalties paid by Promedior to Rice University. Rice University has patents on the use of serum amyloid P (SAP) to inhibit fibrosis; Texas A&M University has patent applications on the use of CD209 ligands to inhibit fibrosis.

inflammation, increased hepatocyte fatty acid synthesis, leading to hepatic steatosis, and eventually fibrosis or cirrhosis.^{3,6} In arteries, dyslipidemia leads to oxidized low-density lipoprotein formation and uptake by macrophages, leading to foam cell formation and vascular wall inflammation (atherosclerosis).⁷⁻⁹ Activated macrophages produce tumor necrosis factor (TNF)- α , which can act either locally or systemically, and this pleiotropic cytokine can directly inhibit insulin signaling, leading to insulin resistance.^{4,6,10} Therefore, treatments that modulate obesity-induced tissue inflammation are an active area of research.¹¹⁻¹³

Monocytes and macrophages are found in every tissue of the body and regulate infection, inflammation, and tissue repair; and they appear to be critical in the development of obesity.¹⁴⁻¹⁷ In the adipose tissue of lean (nonobese) animals and humans, there is a population of tissue macrophages that express receptors and proteins that are thought to be responsible for maintaining a quiescent noninflammatory environment.^{18,19} In obesity, there is an increase in the number of adipose tissue macrophages, by either recruitment from the circulation or local proliferation,^{10,20-22} and these macrophages express proinflammatory proteins and surface receptors.^{18,23} This has led to the hypothesis that targeting macrophages in adipose tissue might be a therapeutic target for obesity-associated inflammation.^{16,19}

Pentraxins are a family of highly conserved systemic proteins that regulate the innate immune system and have a profound effect on the development of inflammation and fibrosis.²⁴⁻²⁶ The pentraxin serum amyloid P (SAP; also called PTX2) reduces neutrophil activation and recruitment,²⁷⁻²⁹ inhibits the differentiation of monocytes into fibroblast-like cells, called fibrocytes,³⁰⁻³² and induces macrophages to secrete the anti-inflammatory cytokine IL-10.³³⁻³⁵ Plasma SAP levels are significantly lower in patients with nonalcoholic fatty liver disease compared with controls without nonalcoholic fatty liver disease, and decline further in patients with advanced fibrosis.³⁶ In animal models and two human trials, SAP injections decrease inflammation and fibrosis in multiple organ systems.^{26,32,37-40}

SAP inhibits inflammation and fibrosis and promotes disease resolution by activating the high-affinity IgG receptor Fc γ receptor I (Fc γ RI; CD64)^{33,41-44} and the dendritic cell-specific intercellular adhesion molecule-3-grabbing nonintegrin (DC-SIGN; CD209), a C-type lectin, which binds mannosylated and fucosylated proteins.^{42,45-47} CD209 activation by a synthetic ligand⁴⁸ can mimic SAP effects on neutrophils, monocytes, and macrophages.⁴²

In this report, we show that both SAP and a DC-SIGN ligand (1866) modulate the immune system in diet-induced obesity. SAP and 1866 reduced high-fat diet (HFD)-induced adipose and liver tissue and inflammation, adipocyte differentiation, and the abnormal retention of lipids within hepatocytes (liver steatosis). These

findings suggest that SAP and 1866 might be useful as therapeutics to regulate the innate immune system activation in obesity.

Materials and Methods

Mouse Model of Obesity

All procedures were performed with specific approval of the Texas A&M University (College Station, TX) institutional animal care and use committee. Animals were housed with a 12-hour/12-hour light-dark cycle with free access to food and water. Male C57BL/6 (Jackson Laboratory, Farmington, CT) or *Apcs*^{-/-} SAP knockout (KO)^{29,49} mice, aged 12 to 16 weeks, were fed standard rodent chow (15% kcal fat; Teklad 8604; Envigo, Madison WI), a low-fat diet (10% kcal fat; D12450B formula; Research Diets, New Brunswick, NJ), or a high-fat diet (60% kcal fat; D12492 formula; Research Diets). For low- and high-fat diets, mice were placed on the specified diets for 6 weeks before start of treatment. Mice were given i.p. injections of 20 mmol/L sodium phosphate, pH 7.2, buffer only, 10 mg/kg SAP (EMD-Millipore, Burlington, MA), buffer exchanged to 20 mmol/L sodium phosphate to remove sodium azide, as previously described,⁵⁰ or 0.1 mg/kg CD209 ligand 1866 (5931866; ChemBridge Corp., San Diego, CA), dissolved in 20 mmol/L sodium phosphate, three times a week, as described previously.^{37,42} For glucose tolerance tests, mice were fasted for 16 hours before i.p. injections of 1.5 g/kg glucose (Amresco, Solon, OH) in phosphate-buffered saline. Blood glucose levels were measured before glucose administration (0 minutes), and at 20, 40, 60, 90, and 120 minutes after the injection using commercial blood glucose test strips (CVS Pharmacy, Woonsocket, RI). Mice were euthanized 35 days after initiation of treatment by asphyxiation with carbon dioxide at 3 L/minute.⁵¹ Mice were randomly assigned to dietary and treatment groups by personnel uninvolved with the study.

Histology and Antibody Staining

After euthanasia, organs, including epididymal white adipose and interscapular brown adipose tissue, liver, spleen, lungs, and kidneys, were weighed before processing for histology. Adipose tissue and liver were fixed in zinc-buffered formalin solution (0.1% ZnSO₄; 4% formaldehyde) for 2 days and then placed in 10% and then 30% sucrose solution in phosphate-buffered saline for 2 days each. Tissues were then kept in 70% ethanol until paraffin processing and sectioning (5 μ m thick). Tissue sections were stained with hematoxylin and eosin, Sirius red to detect collagen, 5 μ g/mL antibodies against Mac2 (clone M3/38; BioLegend, San Diego, CA) to detect tissue macrophages, or 5 μ g/mL antibodies against mitochondrial uncoupling protein 1 [UCP1; GTX112784 (Genetex, Irvine, CA) or NBP2-20796

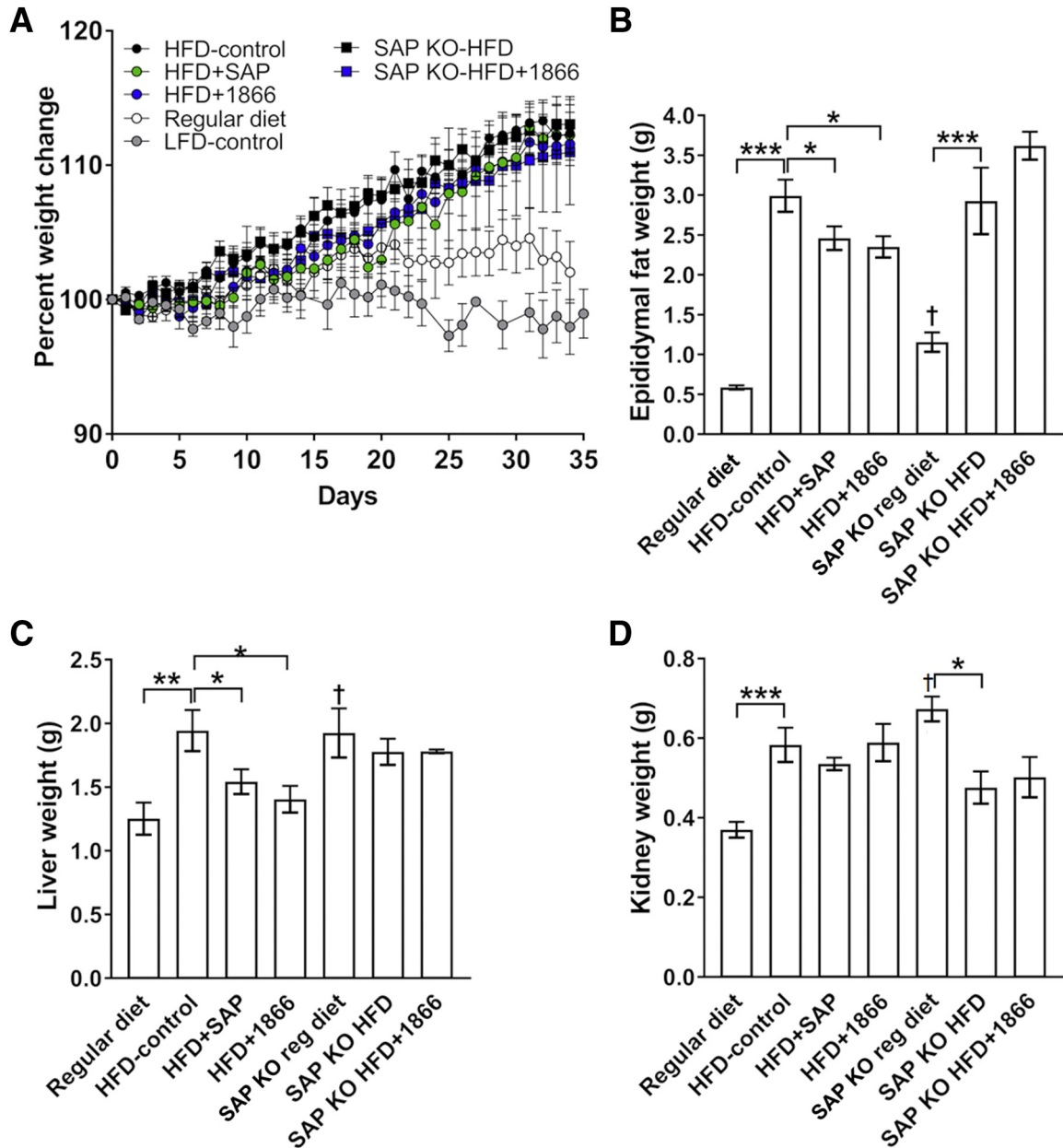


Figure 1 Serum amyloid P (SAP)- and 1866-treated mice have reduction in organ weights. C57BL/6 or SAP knockout (KO) mice were maintained on regular diet, low-fat diet (LFD), or high-fat diet (HFD) for 6 weeks before they were injected three times a week with SAP or 1866 for 35 days. **A:** Body weight of mice in different group over 35 days. **B:** Epididymal white fat. **C:** Liver weight. **D:** Sum of both kidney weights. Data are expressed as means \pm SEM (A–D). $n \geq 6$ mice (A–D). * $P < 0.05$, ** $P < 0.01$, and *** $P < 0.001$ (one-way analysis of variance, Dunnett test); † $P < 0.05$ versus C57BL/6 mice on a regular diet (t -test). reg, regular.

(Novus Biologicals, Littleton, CO) found in brown fat, as described previously.^{37,42,52,53}

Stromal vascular fraction (SVF) cell isolation was performed, as described,⁵⁴ and cell spots were air dried.⁵⁵ Tissue sections and cell spots were stained, as previously described,^{37,42,52,53} with 5 μ g/mL antibodies against CD3 (clone 17A2; BioLegend) to detect T cells, CD11b (clone M1/70; BioLegend) to detect neutrophils and macrophages, CD11c (clone N418; BioLegend) to detect dendritic cells, CD64 (rabbit monoclonal antibody 50086-R001; SinoBiological, Wayne, PA) to detect Fc γ receptor I expression, CD206 (clone MR5D3; BioRad, Hercules, CA) to detect

regulatory macrophages, CD209 (clone eBio22D1; eBioScience—Thermo Fisher Scientific, Waltham, MA) to detect DC-SIGN—expressing cells, Ly6c (clone HK1.4; BioLegend) to detect blood and inflammatory macrophages, Ly6g (clone 1A8; BioLegend) to detect neutrophils, F4/80 (clone Cl:A3-1; BioRad) and Mac2 (clone M3/38; BioLegend) to detect tissue macrophages, and CD45 (30-F11; BioLegend) to detect all leukocytes. Isotype-matched irrelevant rat and hamster (BioLegend) or rabbit (Southern Biotech, Birmingham, AL) antibodies were used as controls. Secondary F(ab')₂ biotin-conjugated donkey anti-rat, anti-hamster, or anti-rabbit antibodies were from Jackson

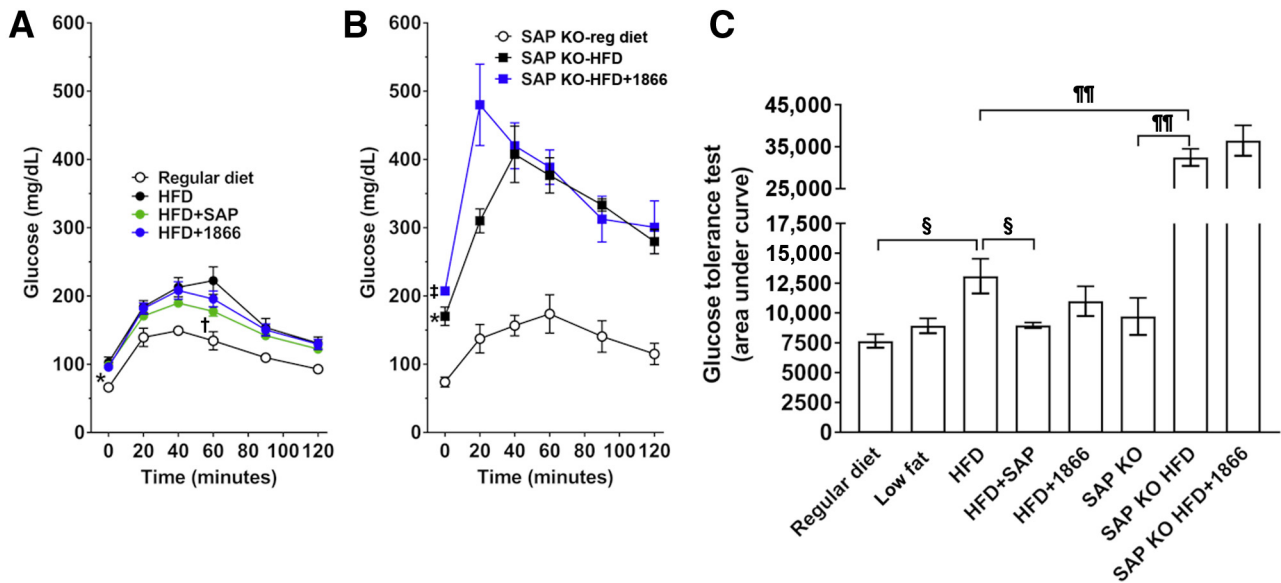


Figure 2 Serum amyloid P (SAP)-treated mice have improved glucose tolerance. C57BL/6 and SAP knockout (KO) mice on regular diet or high-fat diet (HFD) were injected three times a week with SAP or 1866. **A** and **B**: At 35 days, C57BL/6 (**A**) and SAP KO (**B**) mice were fasted overnight and subjected to an i.p. injection of glucose (1.5 g/kg body weight), and tail vein blood samples were assessed for glucose concentration at the indicated times. **C**: Glucose tolerance over 120 minutes was assessed by area under the curve analysis. Data are expressed as means \pm SEM (**A–C**). $n = 3$ to 6 mice (**A–C**). * $P < 0.05$ regular diet versus HFD (one-way analysis of variance, Dunnett test); † $P < 0.05$ HFD+SAP versus HFD alone (one-way analysis of variance, Dunnett test); ‡ $P < 0.05$ SAP Ko-HFD+1866 versus SAP Ko-Reg diet (one-way analysis of variance, Dunnett test); § $P < 0.05$ (one-way analysis of variance, Dunnett test); ¶ $P < 0.01$. reg, regular.

ImmunoResearch (West Grove, PA) or Novus Biologicals; and biotinylated antibodies were revealed with streptavidin-conjugated alkaline phosphatase staining (Vector Laboratories, Burlingame, CA). Commercial kits were used to measure serum levels of cholesterol (MilliporeSigma, St. Louis, MO) and aldosterone (Enzo Life Sciences, Farmingdale, NY), following the manufacturer's instructions.

Stromal Vesicular Cell Culture

SVF cell isolation from epididymal white adipose tissue of C57BL/6 or SAP KO mice on regular diet was performed, as described.⁵⁴ Cells were resuspended at 5×10^4 cells/mL in Dulbecco's modified Eagle's medium (Lonza, Walkersville, MD), containing 10% calf serum (Seradigm-VWR, Radnor, PA), 100 U/mL penicillin, 100 μ g/mL streptomycin, and 2 mmol/L glutamine (Lonza) at 37°C in a humidified 5% CO₂ incubator in 96-well μ -plates (ibidi, Madison, WI). The medium was changed every 2 days. When cells reached approximately 80% confluence, medium was replaced with Dulbecco's modified Eagle's medium containing serum, antibiotics, and 250 ng/mL dexamethasone, 500 ng/mL insulin, and 40 μ g/mL IBMX (all from MilliporeSigma), in the presence or absence of 10 μ g/mL SAP or 1 μ g/mL 1866. After 4 days, supernatants were collected, the cells were air dried, and then the cells were fixed and stained with 5 μ g/mL antiperilipin antibodies (Novus Biologicals), as described.^{37,42,52,53} Oil red O staining was performed, as described.⁵⁶ Supernatants were assessed for IL-10 and IL-12 by enzyme-linked immunosorbent assay (Peprotech, Rocky Hill, NJ).

Image Quantification

Tissue sections, stained with antibodies or Sirius red, were analyzed with ImageJ2 software version 1.52p (NIH, Bethesda, MD; <http://imagej.nih.gov/ij>).⁵⁷ The percentage area of tissue stained with was quantified as a percentage of the total area of the tissue, as described.^{29,37,53} Adipocyte size was calculated using the ImageJ plug-in Adiposoft version 1.16 (Imaging Unit of the Center for Applied Medical Research, University of Navarra, Pamplona, Spain).⁵⁸

Cytokine and SAP Quantification

After euthanasia, blood was collected and serum was clarified by centrifugation at $5000 \times g$ for 5 minutes. Serum was stored at -80°C until analysis. Cytokines were measured with a multiplex assay using fluorescence-encoded beads (Mouse Inflammation 13-plex Panel; BioLegend) and flow cytometry (Accuri C6; BD Biosciences, San Jose, CA), following the manufacturer's instructions. Data were analyzed using LEGENDplex data analysis software version 8.0 (BioLegend), and the concentration of proteins was calculated from standard curves. Murine SAP levels were measured by Western blot analysis, as described previously.^{29,37}

Statistical Analysis

Statistical analysis was performed using Prism version 7 (GraphPad Software, La Jolla, CA). Statistical significance between two groups was determined by *t*-test, or

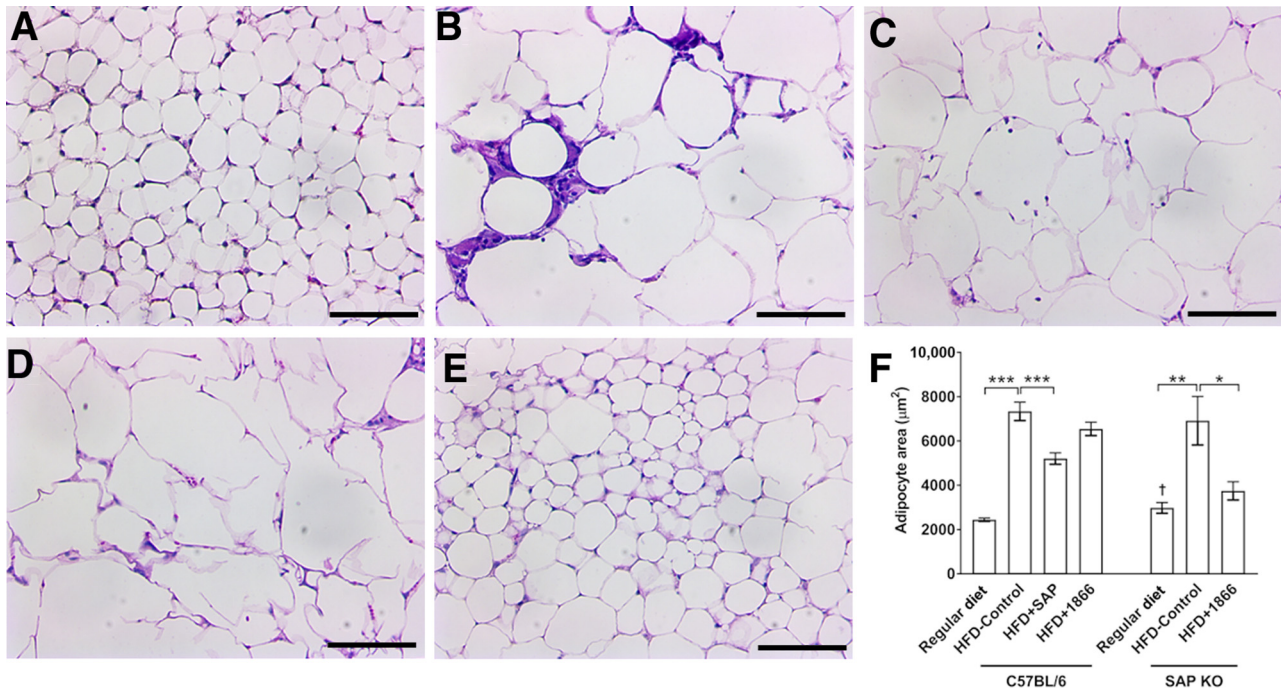


Figure 3 Serum amyloid P (SAP) injections reduce high-fat diet (HFD)–induced changes in white adipose tissue. **A–D**: C57BL/6 mice on regular diet (**A**) or HFD (**B–D**) were injected three times a week with buffer (**B**), SAP (**C**), or 1866 (**D**) for 35 days. **E**: SAP knockout (KO) mice maintained on a regular diet or HFD were injected with buffer or 1866. **A–E**: Representative images of epididymal white fat sections were stained with hematoxylin and eosin. Images are representative of three to eight mice per condition. **F**: Total adipocyte area (μm^2) was calculated. Data are expressed as means \pm SEM (**F**). $n = 3$ to 8 mice per group (**F**). * $P < 0.05$, ** $P < 0.01$, and *** $P < 0.001$ (one-way analysis of variance, Dunnett test); $^{\dagger}P < 0.05$ versus C57BL/6 on regular diet (t -test). Scale bars = 0.1 mm (**A–E**).

between multiple groups using analysis of variance with Dunnett post test, and significance was defined as $P < 0.05$.

Results

SAP and 1866 Decrease High-Fat Diet–Increased Adipose Tissue and Liver Weight

SAP and the DC-SIGN ligand 1866 both inhibit the adhesion, infiltration, and differentiation of leukocytes in multiple models of inflammation and fibrosis.^{28,29,34,37,42,59–61} As obesity is linked with chronic, low-grade inflammation, especially in adipose tissue and liver,^{3,62} it was assessed whether SAP and/or 1866 could attenuate HFD-induced obesity. SAP and 1866 did not significantly affect total weight gain of either C57BL/6 or SAP KO mice on an HFD (**Figure 1A**). Compared with C57BL/6 mice on regular and low-fat diets, C57BL/6 mice on the HFD had significantly increased white fat, liver, and kidney weights (**Figure 1, B–D**, and **Supplemental Figure S1**). Compared with C57BL/6 mice on a regular diet, SAP KO mice on a regular diet had increased white fat, liver, and kidney weights; and compared with SAP KO mice on a regular diet, SAP KO mice on the HFD had significantly increased white fat but reduced kidney weights (**Figure 1, B–D**). Compared with buffer-treated C57BL/6 mice, both SAP and 1866

treatments reduced HFD-induced white fat and liver weight, but did not significantly affect the weight of the kidneys (**Figure 1, B–D**). The 1866 treatments did not alter white fat, liver, and kidney weights in SAP KO mice on the HFD (**Figure 1, B–D**). SAP and 1866 did not significantly affect the total weight or organ weights of C57BL/6 mice on the low-fat diet (**Supplemental Figure S1**). These data suggest that both endogenous SAP and injections of SAP and 1866 can affect organ weights in diet-induced obesity.

SAP Improves Glucose Tolerance and Decreases Aldosterone on a High-Fat Diet

Obesity leads to systemic metabolic dysregulation and type 2 diabetes with an inability to effectively regulate systemic glucose levels.^{3,13} As seen previously,^{17,63} compared with C57BL/6 mice on a regular diet, HFD-maintained mice had a significant increase in basal glucose levels (**Figure 2A**). SAP and 1866 injections did not significantly affect basal glucose levels of C57BL/6 mice on an HFD (**Figure 2A**). Compared with SAP KO mice on a regular diet, SAP KO mice on an HFD had significant increases in basal glucose levels (**Figure 2B**). After a single injection of glucose, all mice had an increase in blood glucose levels (**Figure 2**). Compared with C57BL/6 mice on a regular diet, HFD-fed mice had significantly elevated glucose levels (**Figure 2**). Compared with buffer-treated HFD C57BL/6 mice, SAP,

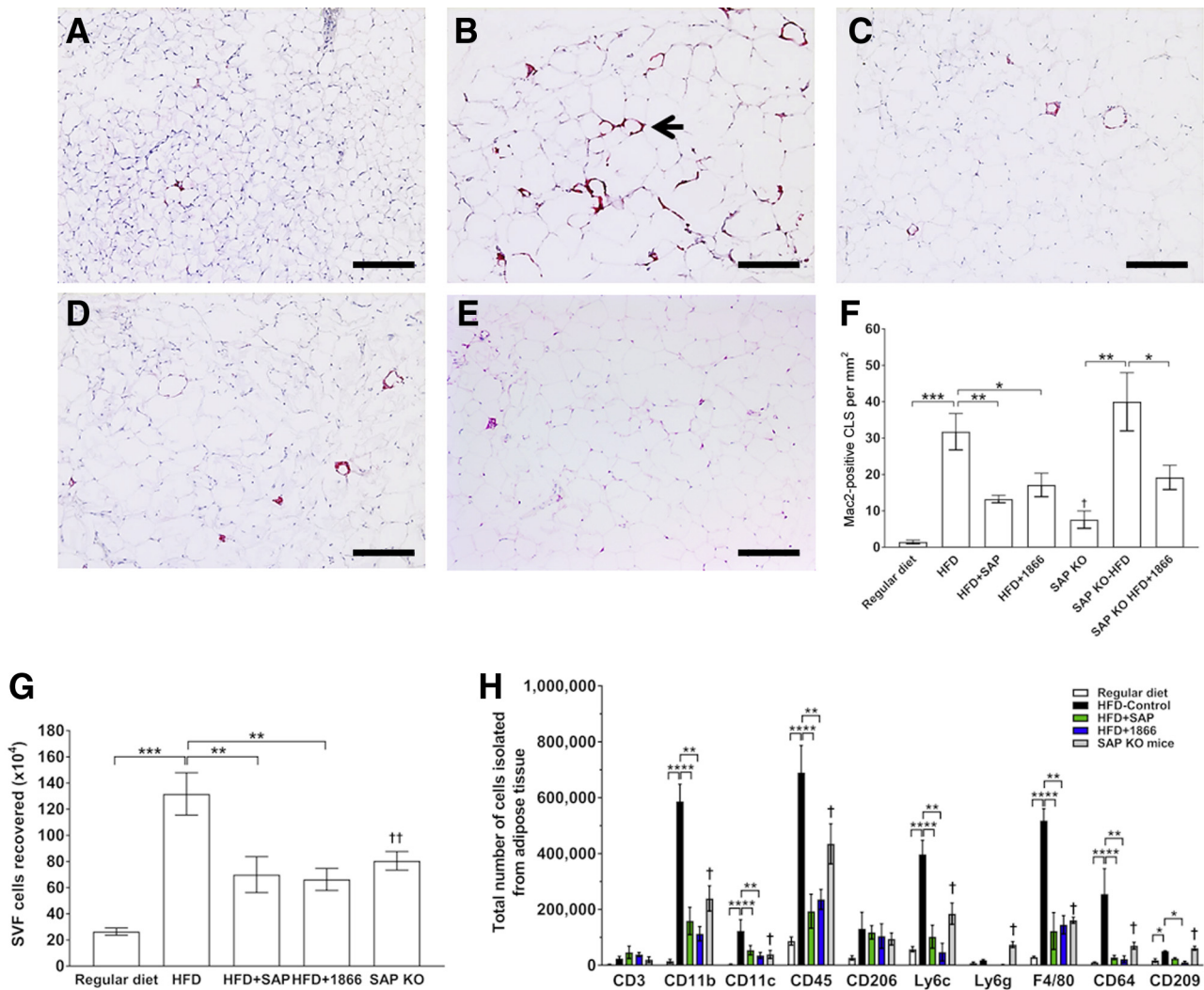


Figure 4 Serum amyloid P (SAP) and 1866 injections reduce high-fat diet (HFD)–induced inflammation in white adipose tissue. **A–D**: Adipose tissue sections from C57BL/6 mice on regular diet (**A**) or HFD (**B–D**), with mice injected three times a week with buffer (**B**), SAP (**C**), or 1866 (**D**). **E**: SAP knock-out (KO) mice were maintained on a regular diet. Representative images of epididymal white fat sections were stained with anti-Mac2 antibodies to detect macrophages in crown-like structures (CLS). **Arrow** indicates CLS. Images are representative of three to seven mice per condition. **F**: Quantification of Mac2-positive CLS. **G** and **H**: Stromal vesicular fraction (SVF) cells of epididymal adipose tissue were isolated, counted (**G**), and stained (**H**) with antibodies for the indicated markers. Data are expressed as means \pm SEM (**F–H**). $n = 3$ to 7 mice per group (**F–H**). * $P < 0.05$, ** $P < 0.01$, and *** $P < 0.001$ versus buffer-treated HFD mice (one-way analysis of variance, Dunnett test); † $P < 0.05$, †† $P < 0.01$ versus C57BL/6 on regular diet (t -test). Scale bars = 0.2 mm (**A–E**).

but not 1866, treated mice had significantly lower serum glucose levels (Figure 2, A and C). In SAP KO mice on the HFD, 1866 treatment did not lower serum glucose levels (Figure 2, B and C). There were no significant differences in serum glucose between mice on a low-fat and regular diet or SAP KO mice on a regular diet (Figure 2C). These data suggest that both endogenous SAP and injections of SAP, but not 1866, can affect glucose metabolism associated with diet-induced obesity.

Diet-induced obesity also leads to elevated levels of serum cholesterol levels,^{64,65} but there was no significant effect of SAP or 1866 on total cholesterol levels in serum for HFD C57BL/6 or SAP KO mice (Supplemental Figure S2A). However, compared with C57BL/6 mice on a regular diet, SAP KO mice on a regular diet had higher total serum

cholesterol levels (Supplemental Figure S2A). Elevated serum aldosterone levels are also associated with obesity⁶⁶; SAP, but not 1866, significantly lowered serum aldosterone levels for HFD mice (Supplemental Figure S2B). In mice, SAP levels increase after systemic inflammation, after potent stimuli, such as injections of lipopolysaccharide, or acute (cecal ligation and puncture), chronic (graft-versus-host disease), or systemic autoimmune disease (MRL/lpr) models,^{67–71} but SAP does not appear to be up-regulated in HFD-treated mice.^{72,73} There was no significant difference in serum SAP levels between C57BL/6 mice fed a regular or high-fat diet (Supplemental Figure S2C). Diet-induced obesity leads to the production of several inflammatory cytokines by adipose tissue macrophages, dendritic cells, and T cells.^{3,74} HFD mice had elevated serum levels of IL-1 β , IL-23, interferon (IFN)- β , IFN- γ ,

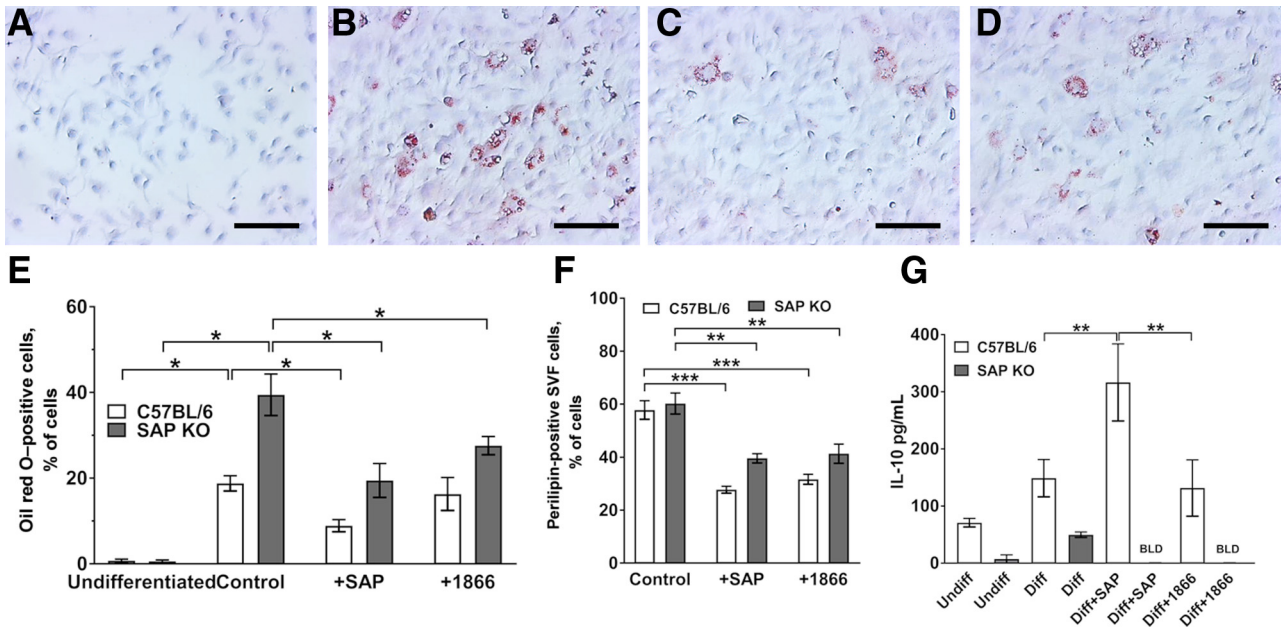


Figure 5 Serum amyloid P (SAP) and 1866 inhibit adipocyte differentiation *in vitro*. Stromal vesicular fraction (SVF) cells isolated from C57BL/6 and SAP knockout (KO) mice on a regular diet were differentiated in the presence or absence of SAP and 1866. **A–D:** Undifferentiated (Undiff; **A**), differentiated (Diff; **B**), or SVF (**C** and **D**) cells differentiated in the presence of SAP (**C**) or 1866 (**D**) were stained with oil red O. Images are representative of three to seven mice per condition. **E** and **F:** Quantification of oil red O–positive (**E**) and perlipin-positive (**F**) cells. **G:** IL-10 production from SVF cells of C57BL/6 and SAP KO mice cultured in the presence or absence of SAP or 1866. Data are expressed as means ± SEM (**E–G**). *n* = 3 to 7 mice per group (**E–G**). **P* < 0.05, ***P* < 0.01, and ****P* < 0.001 (one-way analysis of variance, Dunnett test). Scale bars = 0.2 mm (**A–D**). BLD, below level of detection.

MCP-1, and TNF- α (Supplemental Figure S2D). SAP reduced serum levels of IL-23, IFN- β , MCP-1, and TNF- α , whereas 1866 reduced IFN- γ (Supplemental Figure S2D). These data suggest that SAP and 1866 can affect some systemic factors associated with diet-induced obesity.

SAP Decreases Adipocyte Size and Crown-Like Structures in White Adipose Tissue

Obesity leads to an increase in adipocyte size (hypertrophy) and/or an increase in adipocyte numbers (hyperplasia).^{63,75} Compared with white adipose tissue from regular diet mice, both C57BL/6 and SAP KO mice on the HFD had adipocytes with increased size (Figure 3, A, B, D, and F). Compared with HFD buffer-treated mice, SAP-treated C57BL/6 mice had a significant reduction in adipocyte size (Figure 3, C and F). Conversely, compared with C57BL/6 mice on a regular diet, SAP KO mice on a regular diet had adipocytes with increased size (Figure 3, E and F). Although 1866 did not significantly alter adipocyte size for C57BL/6 mice on the HFD, in SAP KO mice 1866 reduced adipocyte size (Figure 3F and Supplemental Figure S3, A–C). These data suggest that SAP and 1866 can reduce cell size in white adipose tissue.

Although adipose tissue from nonobese mice contains a variety of immune cells, including macrophages, lymphocytes, and neutrophils, the accumulation of inflammatory

cells in obesity may contribute to both local adipocyte tissue dysfunction and drive systemic inflammation.^{3,17} To determine whether SAP and/or 1866 could alter the number or composition of adipose tissue immune cells, cells were assessed in tissue sections. Mac2-positive macrophages that aggregate into crown-like structures (CLS) scavenge lipid droplets and dead adipocytes, and the number of CLS is positively correlated with systemic insulin resistance in obese patients.^{62,76,77} Compared with mice on a regular diet, both C57BL/6 and SAP KO mice on an HFD had a significant increase in the number of Mac2-positive macrophages associated with CLSs (Figure 4, A, B, and F). HFD mice treated with SAP or 1866 had reduced Mac2-positive CLS (Figure 4, C, D, and F). Compared with mice on a regular diet, SAP KO mice on a regular diet had increased numbers of Mac2-positive CLS (Figure 4, E and F). These data suggest that endogenous SAP and injections of SAP or 1866 can regulate macrophage accumulation in white adipose tissue.

To further elucidate the effect of SAP and 1866 on adipose tissue immune cells, SVF cells were isolated from white adipose tissue. Compared with mice on a regular diet, HFD mice had a significant increase in the number of isolated SVF cells (Figure 4G). Treatment of HFD mice with either SAP or 1866 decreased the number of isolated SVF cells (Figure 4G). Conversely, compared with mice on a regular diet, SAP KO mice on a regular diet had increased numbers of SVF cells (Figure 4G). Compared with mice on

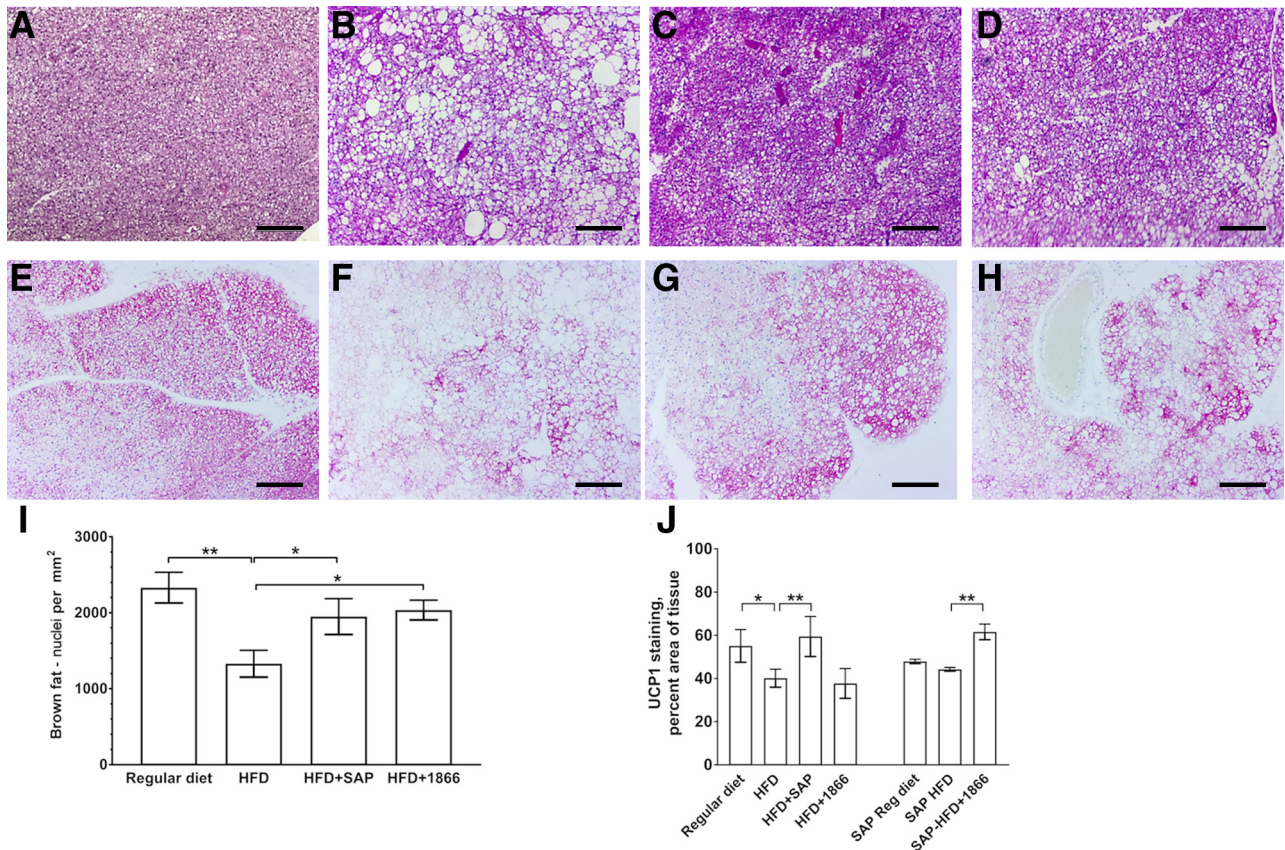


Figure 6 Serum amyloid P (SAP) and 1866 reduce high-fat diet (HFD)—induced changes in brown adipose tissue. **A–H:** C57BL/6 mice on regular diet (**A** and **E**), HFD (**B** and **F**), HFD + SAP (**C** and **G**), or HFD + 1866 (**D** and **H**). **A–H:** Representative images of brown fat sections were stained with hematoxylin and eosin (**A–D**) or anti-uncoupling protein 1 (UCP1) antibodies (**E–H**). Images are representative of three to seven mice per condition. **I:** Number of nuclei per mm². **J:** Quantification of tissue stained with anti-UCP1 antibodies. Data are expressed as means \pm SEM (**I** and **J**). $n = 3$ to 7 mice per group (**I** and **J**). * $P < 0.05$, ** $P < 0.01$ (one-way analysis of variance, Dunnett test). Scale bars = 0.2 mm (**A–H**). reg, regular.

a regular diet, the SVF cells from HFD mice had more CD11b-, CD11c-, CD45-, Ly6c-, F4/80-, CD64-, and CD209-positive cells (Figure 4H). Compared with HFD buffer-treated mice, both SAP- and 1866-treated HFD mice had fewer CD11b-, CD11c-, CD45-, Ly6c-, F4/80-, and CD64-positive SVF cells (Figure 4H). The 1866, but not SAP, reduced CD209-positive SVF cells (Figure 4H). Compared with C57BL/6 mice on a regular diet, SAP KO mice had a significant increase in the number of CD11b-, CD11c-, CD45-, Ly6c-, Ly6g-, F4/80-, CD64-, and CD209-positive SVF cells (Figure 4H). These data suggest that, compared with mice on a regular diet, HFD leads to alteration in the composition of immune cells in adipose tissue, and SAP and 1866 change this composition.

SAP and 1866 Inhibit Adipocyte Differentiation

To determine whether SAP and/or 1866 can directly regulate adipocyte differentiation, we differentiated SVF cells from regular diet C57BL/6 and regular diet SAPKO mice *in vitro* in the presence or absence of SAP or 1866. Compared with undifferentiated SVF cells, an increased percentage of differentiated SVF cells showed positive oil red O staining for

lipids (Figure 5, A, B, and E). Compared with control differentiated SVF cells, SVF cells differentiated in the presence of SAP or 1866 had reduced percentages of oil red O-positive cells (Figure 5, B–E). As with C57BL/6 SVF cells, SAP and 1866 decreased the percentage of oil red-positive SAP KO differentiated SVF cells (Figure 5E). Differentiated SVF cells from mice on a regular diet were also stained for the lipid droplet protein perilipin.⁷⁸ Differentiated C57BL/6 and SAP KO SVF cells had similar percentages of perilipin-positive cells (Figure 5F). Compared with differentiated SVF cells, C57BL/6 and SAP KO SVF cells differentiated in the presence of SAP or 1866 had a reduced percentage of cells with perilipin staining (Figure 5F). SAP and 1866 increase extracellular accumulation of the anti-inflammatory cytokine IL-10 by macrophages,^{33,35,42,79} and the adipocyte-derived cytokine adiponectin protects against obesity in part by inducing IL-10.⁸⁰ Compared with control differentiated SVF cells, SVF cells differentiated in the presence of SAP, but not 1866, had increased IL-10 accumulation (Figure 5G). Although SAP KO-derived SVF cells accumulated IL-10, SAP or 1866 reduced this to undetectable levels (Figure 5G). Undifferentiated SAP KO-derived SVF cells accumulated 3.4 ± 1.4 pg/mL IL-12 (means \pm SEM;

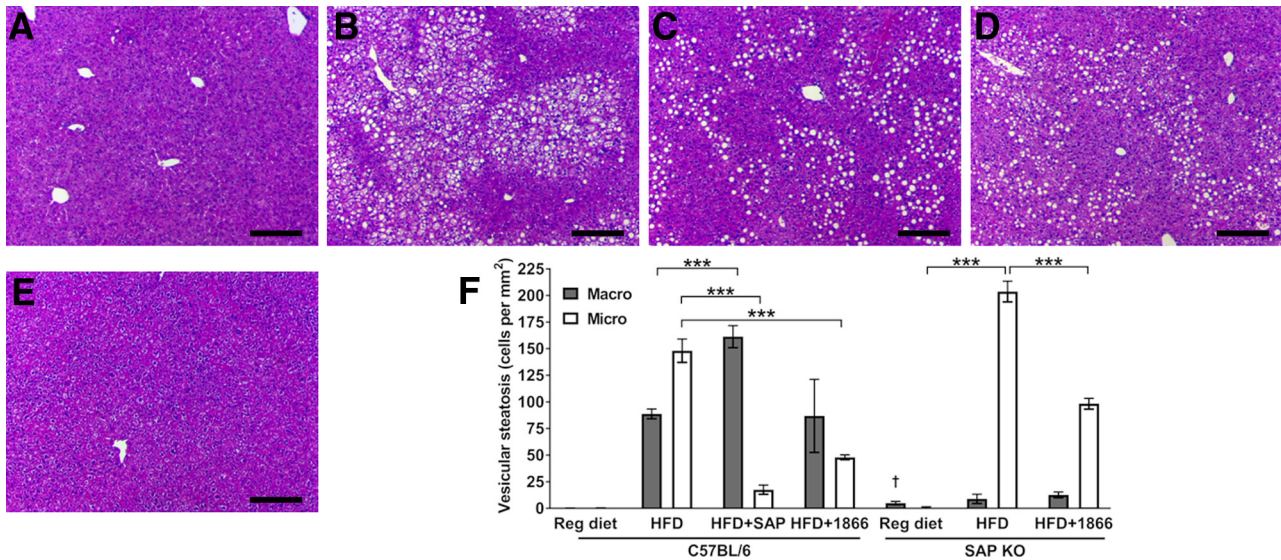


Figure 7 Serum amyloid P (SAP) and 1866 reduce high-fat diet (HFD)–induced changes in liver steatosis. **A–D**: C57BL/6 mice on regular diet (**A**) or HFD (**B–D**) were injected three times a week with buffer (**B**), SAP (**C**), or 1866 (**D**) for 35 days. **E**: SAP knockout (KO) mice were maintained on a regular diet. Images show liver sections stained with hematoxylin and eosin. Images are representative of three to four mice per condition. **F**: The numbers of hepatocytes with macrosteatosis (Macro) or microsteatosis (Micro) were counted. Data are expressed as means \pm SEM (**F**). $n = 3$ to 4 mice per group (**F**). $***P < 0.001$ (one-way analysis of variance, Dunnett test); $^\dagger P < 0.05$ versus C57BL/6 on regular diet (t -test). Scale bars = 0.2 mm (**A–E**). reg, regular.

$n = 4$), differentiated SAP KO SVF cells produced 14.7 ± 4.0 pg/mL IL-12, and SAP KO SVF cells, differentiated in the presence of SAP, produced 8.0 ± 0.9 pg/mL IL-12, indicating that in the latter condition, the SAP KO SVF cells can accumulate extracellular cytokines. Isolated and cultured SVF cells are composed mainly of adipocytes and their precursors and macrophages,^{4,54} and SAP and 1866 regulate monocyte to macrophage differentiation and macrophage priming.^{42,60} Compared with control differentiated C57BL/6 SVF cells, SAP and 1866 increased the percentage of CD206-positive cells; for SAP KO cells, 1866 increased the percentage of CD206-positive cells (Supplemental Figure S4). Together, these data suggest that SAP and 1866 can regulate both adipocyte and macrophage differentiation.

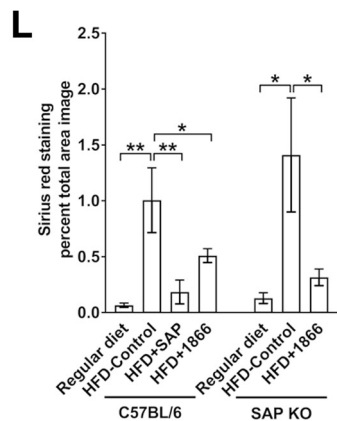
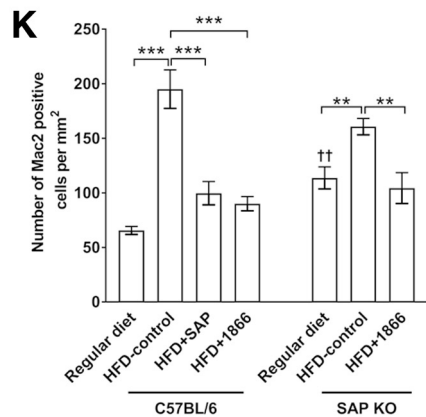
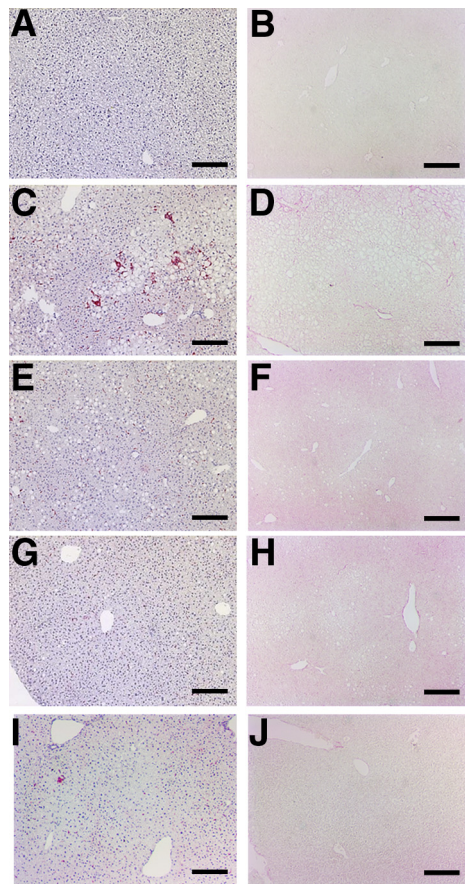
SAP and 1866 Reverse HFD-Induced Changes in Brown Fat and Liver

High-fat diet–induced obesity also leads to changes in brown adipose and liver cell composition.^{3,75} As previously observed,⁸¹ compared with mice on a regular diet, the brown fat of HFD mice had a reduced density of cells and enlarged adipocytes (Figure 6, A, B, and I), and this was also observed for SAP KO mice (Supplemental Figure S3, D–F). Compared with control HFD mice, HFD mice treated with either SAP or 1866 had a higher density of cells in brown adipose tissue (Figure 6, C, D, and I). Brown fat can process lipids and carbohydrate to generate heat (adaptive thermogenesis), and this is mediated by UCP1.^{82,83} There was reduced UCP1 staining of brown fat in HFD C57BL/6 mice (Figure 6, E, F, and J). SAP, but not 1866, reversed this effect (Figure 6, G, H, and J). Although 1866 did not

significantly alter UCP1 staining in the brown fat of C57BL/6 mice on the HFD, in SAP KO mice, 1866 increased UCP1 staining (Figure 6J and Supplemental Figure S3, G–I). These data suggest that SAP can reverse some of the effects of high-fat diet on brown adipose tissue in mice.

Obesity is associated with nonalcoholic fatty liver disease, a spectrum of liver diseases that ranges from simple steatosis (accumulation of fat droplets within the hepatocytes) to hepatitis (inflammation), resulting in nonalcoholic steatosis and ultimately cirrhosis (fibrosis) and liver failure.^{84,85} Compared with regular diet mice, HFD mice had increased macrosteatosis (one single large lipid vacuole within the cell) and microsteatosis (numerous small intracytoplasmic fat vacuoles within the cell) (Figure 7, A, B, and F). Compared with HFD control mice, SAP-treated mice had an increase in macrosteatosis and a reduction in microsteatosis, whereas 1866-treated mice had no significant change in macrosteatosis and a reduction in microsteatosis (Figure 7, C, D, and F, and Supplemental Figure S5, A–C). Compared with C57BL/6 mice on a regular diet, SAP KO mice on a regular diet had a small, but significant, increase in macrosteatosis but no significant change in microsteatosis (Figure 7, E and F). Compared with SAP KO mice on the HFD, 1866-treated SAP KO mice had a reduction in microsteatosis (Figure 7F and Supplemental Figure S5, A–C). In addition, there was a significant change in the ratio of macrosteatosis/microsteatosis between C57BL/6 and SAP KO mice on the HFD (Figure 7F). These data suggest that SAP and 1866 can reverse some of the effects of high-fat diet on liver steatosis.

Obesity is also associated with liver inflammation, especially an increase in macrophages, and liver fibrosis.^{3,86,87}



Compared with normal diet mice, C57BL/6 and SAP KO mice on an HFD had increased numbers of Mac2-positive macrophages, and treatment with SAP or 1866 significantly reduced these numbers (Figure 8, A–D and K, and Supplemental Figure S5, D–F). Conversely, compared with C57BL/6 mice on a regular diet, SAP KO mice on a regular diet had a significant increase in Mac2-positive cells (Figure 8, E and K). Compared with normal diet mice, C57BL/6 and SAP KO mice on an HFD had increased staining with picrosirius red, which detects collagen; and treatment with SAP or 1866 reduced picrosirius red staining (Figure 8, F–I and L, and Supplemental Figure S5, G–I). Compared with C57BL/6 mice on a regular diet, SAP KO mice on a regular diet had no significant change in picrosirius red staining (Figure 8, J and L). These data suggest that SAP and 1866 can attenuate some of the effects of high-fat diet on liver inflammation and fibrosis.

Discussion

Both SAP and the CD209 ligand 1866 could ameliorate multiple aspects of high-fat diet–induced obesity in mice. Both SAP and 1866 appeared to reduce white adipose tissue inflammation, especially the numbers of Mac2-positive macrophages that aggregate into CLSs and inflammatory CD11c- and Ly6C-positive cells. Both SAP and 1866 also reduced the accumulation of lipids in adipocyte cultures and inhibited the accumulation of lipids in brown adipose tissue. SAP, but not 1866, could induce a more rapid reduction in glucose levels after a glucose tolerance test. SAP and 1866 differentially regulated serum cytokine levels; SAP reduced IL-23, MCP-1, IFN- β , and TNF- α , whereas 1866 reduced IFN- γ . In addition, SAP, but not 1866, promoted IL-10 cytokine production in cultured SVF cells. SAP and 1866 differentially regulate liver steatosis. SAP reduced HFD-induced microsteatosis, but increased macrosteatosis, whereas 1866 reduced HFD-induced microsteatosis but did not affect macrosteatosis. SAP knockout mice on a regular diet mirrored many of these findings, including increased white adipocyte size, elevated numbers of inflammatory cells in adipose and liver tissue, and low-grade macrosteatosis; and these effects were exacerbated on a high-fat diet.

Figure 8 Serum amyloid P (SAP) and 1866 reduce high-fat diet (HFD)–induced changes in liver inflammation. **A–H**: C57BL/6 mice on regular diet (**A** and **B**) or HFD (**C–H**) were injected three times a week with buffer (**C** and **D**), SAP (**E** and **F**), or 1866 (**G** and **H**) for 35 days. **I** and **J**: SAP knockout (KO) mice were maintained on a regular diet. **A–J**: Representative images of liver sections were stained with anti-Mac2 antibodies (**A**, **C**, **E**, **G**, and **I**) or Sirius red (**B**, **D**, **F**, **H**, and **J**). Images are representative of three to four mice per condition. **K**: Number of Mac2-positive cells per mm². **L**: Quantification of tissue stained with Sirius red to detect collagen. Data are expressed as means \pm SEM (**K** and **L**). * P < 0.05, ** P < 0.01, and *** P < 0.001 (one-way analysis of variance, Dunnett test); †† P < 0.01 versus C57BL/6 on regular diet (t -test). Scale bars = 0.2 mm (**A–J**).

High-fat diet–induced obesity in animals and humans is associated with elevated levels of a variety of inflammatory cytokines, including IL-1 β , IL-6, IFN- γ , MCP-1, and TNF- α .^{3,4,74} IL-1 β , IL-6, and TNF- α regulate insulin responses by preventing insulin receptor signaling,⁸⁸ alter lipid metabolism,⁸⁹ and promote immune cell migration into adipose tissue.⁴ IL-23, IFN- γ , and MCP-1 all promote proinflammatory conditions associated with obesity by promoting angiogenesis, immune cell recruitment into tissues, and inhibition of anti-inflammatory and proregulatory cells.^{10,74,90} Elevated levels of these cytokines further exacerbate adipose tissue dysfunction and systemic complications, such as type 2 diabetes and liver inflammation. The ability of SAP and 1866 to modulate the levels of cytokines, such as MCP-1 [chemokine (C-C motif) ligand 2], IFN- γ , and TNF- α , suggests that SAP and 1866 may be able to regulate a variety of anti-inflammatory cytokines produced by a range of cell types.

The ability of SAP to induce IL-10 production from SVF cells *in vitro*, and reduce tissue inflammation, is consistent with previous findings showing that SAP reduces neutrophil and monocyte recruitment, fibrocyte differentiation, and macrophage activation in many tissues, and that these processes appear to be dependent on IL-10.^{24–26,33,35} The ability of SAP to regulate glucose levels, adipocyte size, and lipid accumulation in adipose and liver cells could be due to either the effects of SAP on inflammatory cells and cytokine production or a novel direct effect of SAP on pancreatic, adipose, and liver cells. The DC-SIGN (CD209) ligand 1866 mimics the effects of SAP on neutrophil adhesion, macrophage polarization, and bleomycin-induced lung inflammation and fibrosis.⁴² Unlike SAP, 1866 did not reduce HFD-induced adipose cell size or the induction of IL-10 by SVF cell cultures, and had a differential effect on steatosis. SVF cells from SAP KO mice were poor at producing IL-10, although they produced many other cytokines, including IL-12, suggesting that the presence of SAP could be a priming signal for IL-10 accumulation. SAP reduced HFD-induced microsteatosis, and 1866 reduced HFD-induced microsteatosis. Macrosteatosis is considered to have a more favorable clinical outcome with a good long-term prognosis, whereas microsteatosis is associated with a more severe pathology.^{91,92}

SAP regulates cells through CD64 or CD209 receptors, and 1866 is a ligand for CD209.^{42,93} Adipose and liver tissues express these receptors on both immune and nonimmune cells.^{94–99} The ability of SAP and 1866 to modulate adipocytes and liver cells *in vitro* and *in vivo* suggests that SAP and 1866 may act directly on these nonimmune cells to inhibit diet-induced obesity. The observation that SAP, but not 1866, could also modulate glucose levels, induce IL-10 production, and maintain UCP1 levels in brown fat suggests that either CD64 may be a more widely expressed receptor or the cells that express CD64 (either alone or in combination with CD209) are more active in regulating diet-induced obesity.

Fibrotic and inflammatory diseases can be associated with lower circulating levels of SAP, and low levels correlate with disease progression, suggesting that higher SAP levels are beneficial, as is observed in clinical trials.^{30,32,34,36,40} In obese humans, studies indicate that plasma SAP levels are elevated compared with nonobese controls, and correlate with increased cardiovascular disease.^{100–104} However, SAP injections reduce atherosclerosis, and SAP prevents the uptake of low-density lipoproteins, which are associated with obesity and cardiovascular disease.^{8,105,106} This suggests that elevated SAP levels in obese patients may be a mechanism to down-regulate the effects of obesity, rather than a cause of obesity. Together, our results and the work described above suggest the intriguing possibility that a normal function of SAP is to regulate adipose and liver tissue inflammation, that SAP and 1866 are potential therapeutics for high-fat diet–induced inflammation, and that CD64 or CD209 and DC-SIGN are novel targets to reduce obesity-driven inflammation.

Acknowledgments

We thank the animal care staff at Texas A&M for care of animals and Chaodong Wu for helpful discussions.

Supplemental Data

Supplemental material for this article can be found at <http://doi.org/10.1016/j.ajpath.2019.08.005>.

References

1. Hales CM, Carroll MD, Fryar CD, Ogden CL: Prevalence of obesity among adults and youth: United States, 2015–2016. *NCHS Data Brief* 2017, 288:1–8
2. Finkelstein EA, Trogdon JG, Cohen JW, Dietz W: Annual medical spending attributable to obesity: payer- and service-specific estimates. *Health Aff* 2009, 28:w822–w831
3. Lackey DE, Olefsky JM: Regulation of metabolism by the innate immune system. *Nat Rev Endocrinol* 2015, 12:15
4. Crewe C, An YA, Scherer PE: The ominous triad of adipose tissue dysfunction: inflammation, fibrosis, and impaired angiogenesis. *J Clin Invest* 2017, 127:74–82
5. Strissel KJ, Stancheva Z, Miyoshi H, Perfield JW 2nd, DeFuria J, Jick Z, Greenberg AS, Obin MS: Adipocyte death, adipose tissue remodeling, and obesity complications. *Diabetes* 2007, 56:2910–2918
6. Osborn O, Olefsky JM: The cellular and signaling networks linking the immune system and metabolism in disease. *Nat Med* 2012, 18:363
7. Ebong IA, Goff DC Jr, Rodriguez CJ, Chen H, Bertoni AG: Mechanisms of heart failure in obesity. *Obes Res Clin Pract* 2014, 8:e540–e548
8. Xi D, Zhao J, Guo K, Hu L, Chen H, Fu W, Lai W, Guo Z: Serum amyloid P component therapeutically attenuates atherosclerosis in mice via its effects on macrophages. *Theranostics* 2018, 8:3214–3223
9. Woollard KJ, Geissmann F: Monocytes in atherosclerosis: subsets and functions. *Nat Rev Cardiol* 2010, 7:77–86

10. Guzik TJ, Skiba DS, Touyz RM, Harrison DG: The role of infiltrating immune cells in dysfunctional adipose tissue. *Cardiovasc Res* 2017, 113:1009–1023
11. Reilly SM, Chiang S-H, Decker SJ, Chang L, Uhm M, Larsen MJ, Rubin JR, Mowers J, White NM, Hochberg I, Downes M, Yu RT, Liddle C, Evans RM, Oh D, Li P, Olefsky JM, Saltiel AR: An inhibitor of the protein kinases TBK1 and IKK- ϵ improves obesity-related metabolic dysfunctions in mice. *Nat Med* 2013, 19:313
12. Khera R, Murad MH, Chandar AK, Dulai PS, Wang Z, Prokop LJ, Loomba R, Camilleri M, Singh S: Association of pharmacological treatments for obesity with weight loss and adverse events: a systematic review and meta-analysis. *JAMA* 2016, 315:2424–2434
13. Van Gaal L, Dirinck E: Pharmacological approaches in the treatment and maintenance of weight loss. *Diabetes Care* 2016, 39:S260
14. Wynn TA, Chawla A, Pollard JW: Macrophage biology in development, homeostasis and disease. *Nature* 2013, 496:445–455
15. Perdiguero EG, Geissmann F: The development and maintenance of resident macrophages. *Nat Immunol* 2015, 17:2–8
16. Peterson KR, Cottam MA, Kennedy AJ, Hasty AH: Macrophage-targeted therapeutics for metabolic disease. *Trends Pharmacol Sci* 2018, 39:536–546
17. Ivanov S, Merlin J, Lee MKS, Murphy AJ, Guinamard RR: Biology and function of adipose tissue macrophages, dendritic cells and B cells. *Atherosclerosis* 2018, 271:102–110
18. Lumeng CN, Bodzin JL, Saltiel AR: Obesity induces a phenotypic switch in adipose tissue macrophage polarization. *J Clin Invest* 2007, 117:175–184
19. Thomas D, Apovian C: Macrophage functions in lean and obese adipose tissue. *Metabolism* 2017, 72:120–143
20. Weisberg SP, McCann D, Desai M, Rosenbaum M, Leibel RL, Ferrante AW Jr: Obesity is associated with macrophage accumulation in adipose tissue. *J Clin Invest* 2003, 112:1796–1808
21. Amano SU, Cohen JL, Vangala P, Tencerova M, Nicoloro SM, Yawe JC, Shen Y, Czech MP, Aouadi M: Local proliferation of macrophages contributes to obesity-associated adipose tissue inflammation. *Cell Metab* 2014, 19:162–171
22. Keophiphath M, Rouault C, Divoux A, Clement K, Lacasa D: CCL5 promotes macrophage recruitment and survival in human adipose tissue. *Arterioscler Thromb Vasc Biol* 2010, 30:39–45
23. Lauterbach MAR, Wunderlich FT: Macrophage function in obesity-induced inflammation and insulin resistance. *Pflugers Arch* 2017, 469:385–396
24. Du Clos TW: Pentraxins: structure, function, and role in inflammation. *ISRN Inflamm* 2013, 2013:379040
25. Bottazzi B, Inforzato A, Messa M, Barbagallo M, Magrini E, Garlanda C, Mantovani A: The pentraxins PTX3 and SAP in innate immunity, regulation of inflammation and tissue remodelling. *J Hepatol* 2016, 64:1416–1427
26. Cox N, Pilling D, Gomer RH: Serum amyloid P: a systemic regulator of the innate immune response. *J Leukoc Biol* 2014, 96:739–743
27. Maharjan AS, Roife D, Brazill D, Gomer RH: Serum amyloid P inhibits granulocyte adhesion. *Fibrogenesis Tissue Repair* 2013, 6:2
28. Cox N, Pilling D, Gomer RH: Distinct Fc γ receptors mediate the effect of serum amyloid P on neutrophil adhesion and fibrocyte differentiation. *J Immunol* 2014, 193:1701–1708
29. Pilling D, Gomer RH: Persistent lung inflammation and fibrosis in serum amyloid P component (Apc α $-/-$) knockout mice. *PLoS One* 2014, 9:e93730
30. Pilling D, Buckley CD, Salmon M, Gomer RH: Inhibition of fibrocyte differentiation by serum amyloid P. *J Immunol* 2003, 171:5537–5546
31. Peng H, Herzog EL: Fibrocytes: emerging effector cells in chronic inflammation. *Curr Opin Pharmacol* 2012, 12:491–496
32. Verstovsek S, Manshoury T, Pilling D, Bueso-Ramos CE, Newberry KJ, Prijic S, Knez L, Bozinovic K, Harris DM, Spaeth EL, Post SM, Multani AS, Rampal RK, Ahn J, Levine RL, Creighton CJ, Kantarjian HM, Estrov Z: Role of neoplastic monocyte-derived fibrocytes in primary myelofibrosis. *J Exp Med* 2016, 213:1723–1740
33. Castano AP, Lin SL, Surowy T, Nowlin BT, Turlapati SA, Patel T, Singh A, Li S, Lupher ML Jr, Duffield JS: Serum amyloid P inhibits fibrosis through Fc γ R-dependent monocyte-macrophage regulation in vivo. *Sci Transl Med* 2009, 1:5ra13
34. Murray LA, Chen Q, Kramer MS, Hesson DP, Argentieri RL, Peng X, Gulati M, Homer RJ, Russell T, van Rooijen N, Elias JA, Hogaboam CM, Herzog EL: TGF- β driven lung fibrosis is macrophage dependent and blocked by serum amyloid P. *Int J Biochem Cell Biol* 2011, 43:154–162
35. Zhang W, Xu W, Xiong S: Macrophage differentiation and polarization via phosphatidylinositol 3-kinase/Akt–ERK signaling pathway conferred by serum amyloid P component. *J Immunol* 2011, 187:1764–1777
36. Verna EC, Patel J, Bettencourt R, Nguyen P, Hernandez C, Valasek MA, Kisselva T, Brenner DA, Loomba R: Novel association between serum pentraxin-2 levels and advanced fibrosis in well-characterised patients with non-alcoholic fatty liver disease. *Aliment Pharmacol Ther* 2015, 42:582–590
37. Pilling D, Roife D, Wang M, Ronkainen SD, Crawford JR, Travis EL, Gomer RH: Reduction of bleomycin-induced pulmonary fibrosis by serum amyloid P. *J Immunol* 2007, 179:4035–4044
38. Dillingh MR, van den Blink B, Moerland M, van Dongen MGJ, Levi M, Kleinjan A, Wijsenbeek MS, Lupher ML Jr, Harper DM, Getsy JA, Hoogsteden HC, Burggraaf J: Recombinant human serum amyloid P in healthy volunteers and patients with pulmonary fibrosis. *Pulm Pharmacol Ther* 2013, 26:672–676
39. van den Blink B, Dillingh MR, Ginns LC, Morrison LD, Moerland M, Wijsenbeek M, Trehu EG, Bartholmai BJ, Burggraaf J: Recombinant human pentraxin-2 therapy in patients with idiopathic pulmonary fibrosis: safety, pharmacokinetics and exploratory efficacy. *Eur Respir J* 2016, 47:889–897
40. Raghu G, van den Blink B, Hamblin MJ, Brown AW, Golden JA, Ho LA, Wijsenbeek MS, Vasakova M, Pesci A, Antin-Ozerkis DE, Meyer KC, Kreuter M, Santin-Janin H, Mulder GJ, Bartholmai B, Gupta R, Richeldi L: Effect of recombinant human pentraxin 2 vs placebo on change in forced vital capacity in patients with idiopathic pulmonary fibrosis: a randomized clinical trial. *JAMA* 2018, 319:2299–2307
41. Haudek SB, Trial J, Xia Y, Gupta D, Pilling D, Entman ML: Fc receptor engagement mediates differentiation of cardiac fibroblast precursor cells. *Proc Natl Acad Sci U S A* 2008, 105:10179–10184
42. Cox N, Pilling D, Gomer RH: DC-SIGN activation mediates the differential effects of SAP and CRP on the innate immune system and inhibits fibrosis in mice. *Proc Natl Acad Sci U S A* 2015, 112:8385–8390
43. Crawford JR, Pilling D, Gomer RH: Fc γ RI mediates serum amyloid P inhibition of fibrocyte differentiation. *J Leukoc Biol* 2012, 92:699–711
44. Pilling D, Crawford JR, Verbeek JS, Gomer RH: Inhibition of murine fibrocyte differentiation by cross-linked IgG is dependent on Fc γ RI. *J Leukoc Biol* 2014, 96:275–282
45. van Kooyk Y, Geijtenbeek TB: DC-SIGN: escape mechanism for pathogens. *Nat Rev Immunol* 2003, 3:697–709
46. Anthony RM, Wermeling F, Karlsson MC, Ravetch JV: Identification of a receptor required for the anti-inflammatory activity of IVIG. *Proc Natl Acad Sci U S A* 2008, 105:19571–19578
47. Anthony RM, Wermeling F, Ravetch JV: Novel roles for the IgG Fc glycan. *Ann N Y Acad Sci* 2012, 1253:170–180
48. Borrok MJ, Kiessling LL: Non-carbohydrate inhibitors of the lectin DC-SIGN. *J Am Chem Soc* 2007, 129:12780–12785
49. Botto M, Hawkins PN, Bickerstaff MC, Herbert J, Bygrave AE, McBride A, Hutchinson WL, Tennent GA, Walport MJ, Pepys MB: Amyloid deposition is delayed in mice with targeted deletion of the serum amyloid P component gene. *Nat Med* 1997, 3:855–859

50. Shao DD, Suresh R, Vakil V, Gomer RH, Pilling D: Pivotal advance: Th-1 cytokines inhibit, and Th-2 cytokines promote fibrocyte differentiation. *J Leukoc Biol* 2008, 83:1323–1333
51. AVMA: AVMA Guidelines for the Euthanasia of Animals. Schaumburg, IL: American Veterinary Medical Association, 2013
52. Pilling D, Fan T, Huang D, Kaul B, Gomer RH: Identification of markers that distinguish monocyte-derived fibrocytes from monocytes, macrophages, and fibroblasts. *PLoS One* 2009, 4:e7475
53. Karhadkar TR, Pilling D, Cox N, Gomer RH: Sialidase inhibitors attenuate pulmonary fibrosis in a mouse model. *Sci Rep* 2017, 7:15069
54. Church C, Berry R, Rodeheffer MS: Isolation and study of adipocyte precursors. *Methods Enzymol* 2014, 537:31–46
55. Pilling D, Kitas GD, Salmon M, Bacon PA: The kinetics of interaction between lymphocytes and magnetic polymer particles. *J Immunol Methods* 1989, 122:235–241
56. Liu L, Zheng LD, Donnelly SR, Emont MP, Wu J, Cheng Z: Isolation of mouse stromal vascular cells for monolayer culture. *Methods Mol Biol* 2017, 1566:9–16
57. Rueden CT, Schindelin J, Hiner MC, DeZonia BE, Walter AE, Arena ET, Eliceiri KW: ImageJ2: ImageJ for the next generation of scientific image data. *BMC Bioinformatics* 2017, 18:529
58. Galarraga M, Campi6n J, Mu6oz-Barrutia A, Boqu6 N, Moreno H, Mart6nez JA, Milagro F, Ortiz-de-Sol6rzano C: Adiposoft: automated software for the analysis of white adipose tissue cellularity in histological sections. *J Lipid Res* 2012, 53:2791–2796
59. Haudek SB, Xia Y, Huebener P, Lee JM, Carlson S, Crawford JR, Pilling D, Gomer RH, Trial J, Frangogiannis NG, Entman ML: Bone marrow-derived fibroblast precursors mediate ischemic cardiomyopathy in mice. *Proc Natl Acad Sci U S A* 2006, 103:18284–18289
60. Pilling D, Galvis-Carvajal E, Karhadkar TR, Cox N, Gomer RH: Monocyte differentiation and macrophage priming are regulated differentially by pentraxins and their ligands. *BMC Immunol* 2017, 18:30
61. Murray LA, Rosada R, Moreira AP, Joshi A, Kramer MS, Hesson DP, Argentieri RL, Mathai S, Gulati M, Herzog EL, Hogaboam CM: Serum amyloid P therapeutically attenuates murine bleomycin-induced pulmonary fibrosis via its effects on macrophages. *PLoS One* 2010, 5:e9683
62. Lumeng CN, Saltiel AR: Inflammatory links between obesity and metabolic disease. *J Clin Invest* 2011, 121:2111–2117
63. Sun K, Kusminski CM, Scherer PE: Adipose tissue remodeling and obesity. *J Clin Invest* 2011, 121:2094–2101
64. Williams LM, Campbell FM, Drew JE, Koch C, Hoggard N, Rees WD, Kamolrat T, Thi Ngo H, Steffensen IL, Gray SR, Tups A: The development of diet-induced obesity and glucose intolerance in C57BL/6 mice on a high-fat diet consists of distinct phases. *PLoS One* 2014, 9:e106159
65. Barrett P, Mercer JG, Morgan PJ: Preclinical models for obesity research. *Dis Model Mech* 2016, 9:1245
66. Dinh Cat AN, Friederich-Persson M, White A, Touyz RM: Adipocytes, aldosterone and obesity-related hypertension. *J Mol Endocrinol* 2016, 57:F7–F21
67. Zahedi K, Whitehead AS: Acute phase induction of mouse serum amyloid P component: correlation with other parameters of inflammation. *J Immunol* 1989, 143:2880–2886
68. Mortensen RF, Beisel K, Zeleznik NJ, Le PT: Acute-phase reactants of mice, II: strain dependence of serum amyloid P- component (SAP) levels and response to inflammation. *J Immunol* 1983, 130:885–889
69. Bane CE Jr, Ivanov I, Matafonov A, Boyd KL, Cheng Q, Sherwood ER, Tucker EI, Smiley ST, McCarty OJ, Gruber A, Gailani D: Factor XI deficiency alters the cytokine response and activation of contact proteases during polymicrobial sepsis in mice. *PLoS One* 2016, 11:e0152968
70. Bayston KF, Huby R, Cohen J: Sequential measurement of the murine acute-phase protein serum amyloid P component (SAP) as an indicator of graft-versus-host disease following allogeneic bone marrow transplantation in mice. *Clin Exp Immunol* 1990, 81:329–333
71. Rordorf-Adam C, Serban D, Pataki A, Gr6ninger M: Serum amyloid P component and autoimmune parameters in the assessment of arthritis activity in MRL/lpr/lpr mice. *Clin Exp Immunol* 1985, 61:509–516
72. Sundgren NC, Vongpatanasin W, Boggan BM, Tanigaki K, Yuhanna IS, Chambliss KL, Mineo C, Shaul PW: IgG receptor FcγRIIB plays a key role in obesity-induced hypertension. *Hypertension* 2015, 65:456–462
73. Tanigaki K, Sacharidou A, Peng J, Chambliss KL, Yuhanna IS, Ghosh D, Ahmed M, Szalai AJ, Vongpatanasin W, Mattrey RF, Chen Q, Azadi P, Lingvay I, Botto M, Holland WL, Kohler JJ, Sirsi SR, Hoyt K, Shaul PW, Mineo C: Hyposialylated IgG activates endothelial IgG receptor FcγRIIB to promote obesity-induced insulin resistance. *J Clin Invest* 2018, 128:309–322
74. McLaughlin T, Ackerman SE, Shen L, Engleman E: Role of innate and adaptive immunity in obesity-associated metabolic disease. *J Clin Invest* 2017, 127:5–13
75. Sanchez-Gurmaches J, Hung C-M, Guertin DA: Emerging complexities in adipocyte origins and identity. *Trends Cell Biol* 2016, 26:313–326
76. Shaul ME, Bennett G, Strissel KJ, Greenberg AS, Obin MS: Dynamic, M2-like remodeling phenotypes of CD11c+ adipose tissue macrophages during high-fat diet-induced obesity in mice. *Diabetes* 2010, 59:1171–1181
77. Bremer AA, Devaraj S, Afify A, Jialal I: Adipose tissue dysregulation in patients with metabolic syndrome. *J Clin Endocrinol Metab* 2011, 96:E1782–E1788
78. Sztalryd C, Brasaemle DL: The perilipin family of lipid droplet proteins: gatekeepers of intracellular lipolysis. *Biochim Biophys Acta* 2017, 1862:1221–1232
79. Lu J, Marnell LL, Marjon KD, Mold C, Du Clos TW, Sun PD: Structural recognition and functional activation of FcγR by innate pentraxins. *Nature* 2008, 456:989–992
80. Ohashi K, Parker JL, Ouchi N, Higuchi A, Vita JA, Gokce N, Pedersen AA, Kalthoff C, Tullin S, Sams A, Summer R, Walsh K: Adiponectin promotes macrophage polarization toward an anti-inflammatory phenotype. *J Biol Chem* 2010, 285:6153–6160
81. Alcal6 M, Calderon-Dominguez M, Bustos E, Ramos P, Casals N, Serra D, Viana M, Herrero L: Increased inflammation, oxidative stress and mitochondrial respiration in brown adipose tissue from obese mice. *Sci Rep* 2017, 7:16082
82. Richard D, Picard F: Brown fat biology and thermogenesis. *Front Biosci (Landmark Ed)* 2011, 16:1233–1260
83. Seale P: Brown adipose tissue biology and therapeutic potential. *Front Endocrinol (Lausanne)* 2013, 4:14
84. Chalasani N, Younossi Z, Lavine JE, Charlton M, Cusi K, Rinella M, Harrison SA, Brunt EM, Sanyal AJ: The diagnosis and management of nonalcoholic fatty liver disease: practice guidance from the American Association for the Study of Liver Diseases. *Hepatology* 2017, 67:328–357
85. Sumida Y, Yoneda M: Current and future pharmacological therapies for NAFLD/NASH. *J Gastroenterol* 2018, 53:362–376
86. Brempelis KJ, Crispe IN: Infiltrating monocytes in liver injury and repair. *Clin Transl Immunology* 2016, 5:e113
87. Takahashi Y, Fukusato T: Histopathology of nonalcoholic fatty liver disease/nonalcoholic steatohepatitis. *World J Gastroenterol* 2014, 20:15539–15548
88. Hotamisligil GS, Shargill NS, Spiegelman BM: Adipose expression of tumor necrosis factor-α: direct role in obesity-linked insulin resistance. *Science* 1993, 259:87–91
89. Trujillo ME, Sullivan S, Harten I, Schneider SH, Greenberg AS, Fried SK: Interleukin-6 regulates human adipose tissue lipid metabolism and leptin production in vitro. *J Clin Endocrinol Metab* 2004, 89:5577–5582
90. Granata M, Skarmoutsou E, Trovato C, Rossi GA, Mazzarino MC, D'Amico F: Obesity, type 1 diabetes, and psoriasis: an autoimmune triple flip. *Pathobiology* 2017, 84:71–79

91. Tandra S, Yeh MM, Brunt EM, Vuppalanchi R, Cummings OW, Únalp-Arida A, Wilson LA, Chalasani N: Presence and significance of microvesicular steatosis in nonalcoholic fatty liver disease. *J Hepatol* 2011, 55:654–659
92. Softic S, Gupta MK, Wang G-X, Fujisaka S, O'Neill BT, Rao TN, Willoughby J, Harbison C, Fitzgerald K, Ilkayeva O, Newgard CB, Cohen DE, Kahn CR: Divergent effects of glucose and fructose on hepatic lipogenesis and insulin signaling. *J Clin Invest* 2017, 127:4059–4074
93. Lu J, Marjon KD, Mold C, Du Clos TW, Sun PD: Pentraxins and Fc receptors. *Immunol Rev* 2012, 250:230–238
94. Fujisaka S, Usui I, Kanatani Y, Ikutani M, Takasaki I, Tsuneyama K, Tabuchi Y, Bukhari A, Yamazaki Y, Suzuki H, Senda S, Aminuddin A, Nagai Y, Takatsu K, Kobayashi M, Tobe K: Teli-sartan improves insulin resistance and modulates adipose tissue macrophage polarization in high-fat-fed mice. *Endocrinology* 2011, 152:1789–1799
95. Cho KW, Zamarron BF, Muir LA, Singer K, Porsche CE, DelProposto JB, Geletka L, Meyer KA, O'Rourke RW, Lumeng CN: Adipose tissue dendritic cells are independent contributors to obesity-induced inflammation and insulin resistance. *J Immunol* 2016, 197:3650–3661
96. Xu X, Grijalva A, Skowronski A, van Eijk M, Serlie MJ, Ferrante AW Jr: Obesity activates a program of lysosomal-dependent lipid metabolism in adipose tissue macrophages independently of classic activation. *Cell Metab* 2013, 18:816–830
97. Kratz M, Coats BR, Hisert KB, Hagman D, Mutskov V, Peris E, Schoenfelt KQ, Kuzma JN, Larson I, Billing PS, Landerholm RW, Crouthamel M, Gozal D, Hwang S, Singh PK, Becker L: Metabolic dysfunction drives a mechanistically distinct proinflammatory phenotype in adipose tissue macrophages. *Cell Metab* 2014, 20:614–625
98. Ikarashi M, Nakashima H, Kinoshita M, Sato A, Nakashima M, Miyazaki H, Nishiyama K, Yamamoto J, Seki S: Distinct development and functions of resident and recruited liver Kupffer cells/macrophages. *J Leukoc Biol* 2013, 94:1325–1336
99. Gautier EL, Shay T, Miller J, Greter M, Jakubzick C, Ivanov S, Helft J, Chow A, Elpek KG, Gordonov S, Mazloom AR, Ma'ayan A, Chua W-J, Hansen TH, Turley SJ, Merad M, Randolph GJ: Gene-expression profiles and transcriptional regulatory pathways that underlie the identity and diversity of mouse tissue macrophages. *Nat Immunol* 2012, 13:1118–1128
100. Jenny NS, Arnold AM, Kuller LH, Tracy RP, Psaty BM: Serum amyloid P and cardiovascular disease in older men and women: results from the Cardiovascular Health Study. *Arterioscler Thromb Vasc Biol* 2007, 27:352–358
101. Oberbach A, Blüher M, Wirth H, Till H, Kovacs P, Kullnick Y, Schlichting N, Tomm JM, Rolle-Kampczyk U, Murugaiyan J, Binder H, Dietrich A, von Bergen M: Combined proteomic and metabolomic profiling of serum reveals association of the complement system with obesity and identifies novel markers of body fat mass changes. *J Proteome Res* 2011, 10:4769–4788
102. van Dijk SJ, Feskens EJ, Heidema AG, Bos MB, van de Rest O, Geleijnse JM, de Groot LC, Muller M, Afman LA: Plasma protein profiling reveals protein clusters related to BMI and insulin levels in middle-aged overweight subjects. *PLoS One* 2010, 5:e14422
103. Tan Y, Liu TR, Hu SW, Tian D, Li C, Zhong JK, Sun HG, Luo TT, Lai WY, Guo Z-G: Acute coronary syndrome remodels the protein cargo and functions of high-density lipoprotein subfractions. *PLoS One* 2014, 9:e94264
104. Anwer M, Iqbal MJ: Serum amyloid P and endocrine markers in a cohort of obese children. *Indian J Endocrinol Metab* 2018, 22:683–688
105. Li X-A, Yutani C, Shimokado K: Serum amyloid P component associates with high density lipoprotein as well as very low density lipoprotein but not with low density lipoprotein. *Biochem Biophys Res Commun* 1998, 244:249–252
106. Stewart CR, Tseng AA, Mok Y-F, Staples MK, Schiesser CH, Lawrence LJ, Varghese JN, Moore KJ, Howlett GJ: Oxidation of low-density lipoproteins induces amyloid-like structures that are recognized by macrophages. *Biochemistry* 2005, 44:9108–9116